Mechanics Research Communications 103 (2020) 103472

Contents lists available at ScienceDirect

Mechanics Research Communications

journal homepage: www.elsevier.com/locate/mechrescom

Enhanced thermal rectification in graded Si_cGe_{1-c} alloys

I. Carlomagno[a], V.A. Cimmelli[b,*], D. Jou[c,d]

[a] Department of Industrial Engineering, University of Salerno, Via Giovanni Paolo II, 132, 84084, Fisciano, Italy
[b] Department of Mathematics, Computer Science and Economics, University of Basilicata, Viale dell'Ateneo Lucano, 10, 85100, Potenza, Italy
[c] Institut d'Estudis Catalans, Carme 47, Barcelona 08001, Catalonia, Spain
[d] Departament de Física, Universitat Autònoma de Barcelona, 08193 Bellaterra, Catalonia, Spain

ARTICLE INFO

Article history:
Received 16 November 2019
Revised 13 December 2019
Accepted 2 January 2020
Available online 9 January 2020

Keywords:
Heat rectification
Thermal diode
Graded material
Si/Ge alloys

ABSTRACT

We evaluate the rectification coefficient of the heat flux in graded Si_cGe_{1-c} alloys, both for longitudinal heat flow along a direction z and radial heat flow along a direction r, and for linear stoichiometric spatial distributions $c(z)$ and $c(r)$, with $c \in [0, 1]$. To this end, we take an expression for the thermal conductivity $\lambda(c, T)$ fitting the experimental data in the whole interval $0 \le c \le 1$, for different values of the temperature T. Such an expression leads to a highly nonlinear evolution equation for the temperature. It turns out that the systems under consideration are very efficient as thermal rectifier in the full stoichiometric range, and can be used as thermal diode.

1. Introduction

Graded Si/Ge alloys, with composition c changing along the length of the system, have many practical applications in heat transfer problems [1–6]. One of them is heat rectification, namely, the fact that a same difference of temperature but applied in opposite verses along the same direction, generates different heat flows. Such a possibility represents one of the basic features of phononics [7–10], as it provides the theoretical basis for the construction of phononic diodes. This phenomenon arises, for instance, in binary alloys with thermal conductivity depending on a stoichiometric variable c related to the concentration of the different constituents. Thus, thermal rectification is expected in systems changing their composition as, for instance, Si_cGe_{1-c} [11–15], with the stoichiometric composition parameter c gradually changing as a function of the position. The aim of this paper is to analyze in deeper detail heat rectification in Si_cGe_{1-c} nanowires. Hence, first we take an expression for the thermal conductivity $\lambda(c, T)$ fitting the experimental data in the whole interval $0 \le c \le 1$ at several temperatures, which leads to a highly nonlinear evolution equation for the temperature. We explore the consequences of the variable composition on the value of the rectification coefficient $R[c, T_H, T_C]$, with T_H and T_C the hottest and coldest temperatures, respectively, applied to the ends of the nanowire, and R defined as the ratio of the absolute value q_r of the reverse heat flux with respect to a given reference verse, over the absolute value q_d of the direct heat flux with respect to the same verse, i.e., $R[c, T_H, T_C] \equiv q_r/q_d$ [7–10], for given values of T_H and T_C and for a given spatial distribution c. We consider this phenomenon not only for longitudinal heat flow along a nanowire but also for radial heat flow across a cylindrical device with internal radius r_{int} and external radius r_{ext}. In this situation, the material inhomogeneity in the composition is superposed to a geometrical inhomogeneity in the transversal area of the system. We explore the combined consequences of both factors on the value of the rectification coefficient. The paper presents the following layout. In Section 2, we derive a constitutive equation for the thermal conductivity $\lambda(c, T)$ of Si_cGe_{1-c} alloys based on experimental data. In Section 3, we solve the stationary temperature equation in two one-dimensional systems of length $L = 100$ nm and $L = 30$ nm, respectively, and use this solution to obtain the values of the rectification coefficient for different values of the applied heat flux. In Section 4, we consider two cylindrical systems, whose section is constituted by a annulus of radius $R_a \equiv r_{ext} - r_{int} = 100$ nm, and $R_a \equiv r_{ext} - r_{int} = 30$ nm, with r_{ext} and r_{int} the external and internal radius, respectively. For such systems, under the hypothesis of radial heat flow along the direction r, we calculate the corresponding heat rectification coefficient. In Section 5, we discuss the results and their possible extensions.

2. Thermal conductivity of Si_cGe_{1-c} alloys

2.1. Best fit of thermal conductivity

Let us consider a Si_cGe_{1-c} alloy, whose composition c changes along a given direction z. For the sake of illustration, in Table 1 we

* Corresponding author. Tel.:+39 0971205885.
E-mail addresses: isabellacarlomagno85@gmail.com (I. Carlomagno), vito.cimmelli@unibas.it (V.A. Cimmelli), david.jou@uab.cat (D. Jou).

https://doi.org/10.1016/j.mechrescom.2020.103472
0093-6413/

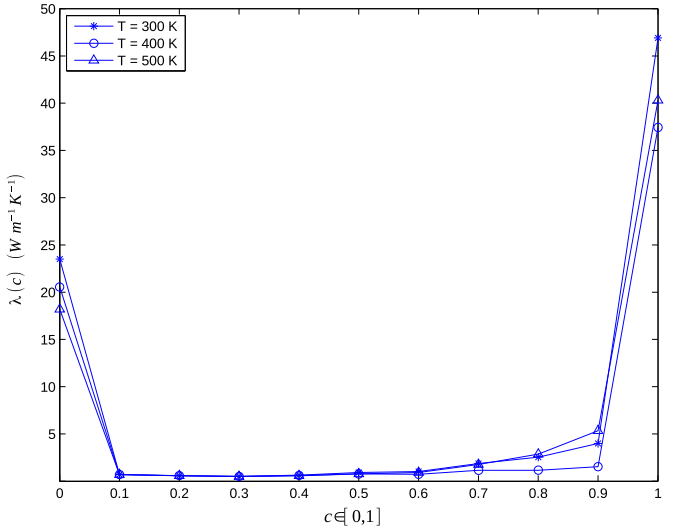

Fig. 1. Sketch of thermal conductivity of a Si_cGe_{1-c} nanowire of length L = 100 nm in terms of c, at $T = 300$ K, $T = 400$ K, and $T = 500$ K.

Table 1
Values of the thermal conductivity (in $Wm^{-1}K^{-1}$) corresponding to the mentioned compositions at $T = 300$ K, $T = 400$ K and $T = 500$ K, for bulk systems, (from [16–19]).

	λ_{Si}	$\lambda_{Si_{0.9}Ge_{0.1}}$	$\lambda_{Si_{0.1}Ge_{0.9}}$	λ_{Ge}
$T = 300$ K	149.95	25.13	10.46	77.95
$T = 400$ K	113.54	23.90	10.06	59.42
$T = 500$ K	92.01	22.79	9.69	48.08

Table 2
Values of the parameters in the analytical expression (1) of thermal conductivity in terms of the composition for a Si_cGe_{1-c} alloy, L = 100 nm [21].

	A	B	D	E	F	G
$T = 300$ K	1.348	6.38	−5.363	22.145	252.53	−251.94
$T = 400$ K	1.331	6.305	−5.282	19.181	239.73	−239.15
$T = 500$ K	1.309	6.208	−5.1836	16.851	228.19	−227.63

give the values of the thermal conductivity for four compositions and three temperatures.

In Fig. 1 it is shown the plot of the function $\lambda(c, T)$ for Si_cGe_{1-c} at $T = 300$ K (*), $T = 400$ K (○), and $T = 500$ K (△), for L = 100 nm, which has been obtained in [4] by using the results in [16–18].

The variation of λ with c is steepest in the ranges $0 \le c \le 0.1$ and $0.9 \le c \le 1$ since a small amount of impurities of different mass strongly contributes to phonon scattering, thus reducing very much thermal conductivity as compared with the corresponding pure system [20]. In Ref. [21] it has been proved that the behavior above of the heat conductivity $\lambda(c, T)$, as a function of the composition c and the temperature T, can be expressed analytically as sum of exponential functions. In particular, the following constitutive equation for $\lambda(c, T)$ was derived:

$$\lambda(c) = Ae^{Bc^2+Dc} + Ee^{Fc^2+Gc} \tag{1}$$

where A, B, D, E, F, G, are suitable temperature-dependent parameters whose values at the constant temperatures $T = 300$ K, $T = 400$ K, $T = 500$ K, are shown in Table 2 and in Table 3 (for Si_cGe_{1-c} and $Si_{1-c}Ge_c$ nanowires, respectively, of length L = 100 nm) and in Table 4 and in Table 5 (for Si_cGe_{1-c} and $Si_{1-c}Ge_c$ nanowires, respectively, of lengt L = 30 nm).

Table 3
Values of the parameters in the analytical expression (1) of thermal conductivity in terms of the composition for a $Si_{1-c}Ge_c$ alloy, L = 100 nm [21].

	A	B	D	E	F	G
$T = 300$ K	3.73	6.38	−7.3978	39.858	252.524	−253.11
$T = 400$ K	3.70	6.305	−7.327	34.465	239.737	−240.32
$T = 500$ K	3.64	6.207	−7.232	29.761	228.197	−228.77

Table 4
Values of the parameters in the analytical expression (1) of thermal conductivity in terms of the composition for a Si_cGe_{1-c} alloy, L = 30 nm [21].

	A	B	D	E	F	G
$T = 300$ K	0.92	6.285	−5.28	12.07	229.09	−228.44
$T = 400$ K	0.897	6.21	−5.18	10.98	213.04	−212.48
$T = 500$ K	0.888	6.15	−5.12	10.17	206.72	−206.17

Table 5
Values of the parameters in the analytical expression (1) of thermal conductivity in terms of the composition for a $Si_{1-c}Ge_c$ alloy, L = 30 nm [21].

	A	B	D	E	F	G
$T = 300$ K	2.50	6.285	−7.29	22.96	229.09	−229.73
$T = 400$ K	2.51	6.21	−7.24	19.18	213.04	−213.59
$T = 500$ K	2.49	6.15	−7.18	17.65	206.73	−207.28

Table 6
Values of the coefficients a_i, b_i, d_i, e_i, f_i and g_i for a Si_cGe_{1-c} alloy, L = 100 nm.

a_1	a_2	b_1	b_2
−0.000145	-2.5×10^{-7}	−0.00064	-1.1×10^{-6}
d_1	d_2	e_1	e_2
0.000723	8.7×10^{-7}	−0.03281	0.0000317
f_1	f_2	g_1	g_2
−0.1343	0.000063	0.13425	−0.0000635

2.2. Temperature dependence of material parameters

As far as the dependence of material parameters on the temperature, we take a series expansion of them around the room temperature, namely $T = 300$ K, up to the second order in T. For the sake of illustration, we show the procedure for $A(T)$ in the case of a Si_cGe_{1-c} alloy, with $L = 100$ nm. We write

$$A(T) = A(300) + a_1(T - 300) + a_2(T - 300)^2 \tag{2}$$

In this way, taking into account the values of A in Table 2, we get

$$A(400) = 1.348 + a_1(100) + a_2(100)^2 = 1.331 \tag{3}$$

$$A(500) = 1.348 + a_1(200) + a_2(200)^2 = 1.309 \tag{4}$$

The linear system (3)-(4) allows the determination of the coefficients a_1 and a_2. Such a procedure can be repeated for the parameters B, D, E, F, and G too, both for L = 100 nm and L = 30 nm, and both for Si_cGe_{1-c} and $Si_{1-c}Ge_c$. The results are shown in the Tables from 6 to 9. In these tables, b_i, d_i, e_i, f_i and g_i respectively correspond to the expansion of the coefficients B, D, E, F, and G in terms of T analogous to a_i in the expansion (2) of coefficient $A(T)$.

In this way we can express the thermal conductivity as function of c and T for all the systems of interest. It is worth observing that the procedure illustrated so far does not depend on the geometry of the system, and hence the fit in (1) can be applied, with the same values of the parameters A, B, D, E, F, and G determined above, to systems with radial symmetry, with $R_a = 100$ nm and $R_a = 30$ nm.

Table 7
Values of the coefficients a_i, b_i, d_i, e_i, f_i and g_i for a $Si_{1-c}Ge_c$ alloy, L = 100 nm.

a_1	a_2	b_1	b_2
−0.00015	-1.5×10^{-6}	−0.000635	-1.15×10^{-6}
d_1	d_2	e_1	e_2
0.000587	1.21×10^{-6}	−0.057375	0.00003445
f_1	f_2	g_1	g_2
−0.134105	0.00006235	0.1341	−0.000062

Table 8
Values of the coefficients a_i, b_i, d_i, e_i, f_i and g_i for a Si_cGe_{1-c} alloy, L = 30 nm.

a_1	a_2	b_1	b_2
−0.0003	7×10^{-7}	−0.000825	7.5×10^{-7}
d_1	d_2	e_1	e_2
0.0012	-2×10^{-6}	−0.0123	0.000014
f_1	f_2	g_1	g_2
−0.20915	0.0004865	0.20785	−0.0004825

Table 9
Values of the coefficients a_i, b_i, d_i, e_i, f_i and g_i for a $Si_{1-c}Ge_c$ alloy, L = 30 nm.

a_1	a_2	b_1	b_2
0.00025	-1.5×10^{-6}	−0.000825	7.5×10^{-7}
d_1	d_2	e_1	e_2
0.00045	5×10^{-7}	−0.04905	0.0001125
f_1	f_2	g_1	g_2
−0.2092	0.000487	0.00586545	0.00155535

3. Rectification of the heat flux in nanowires

3.1. Temperature profiles

In the present section we carry out a computational analysis of heat transport along the direction z in Si_cGe_{1-c} nanowires (direct heat flux) and along $Si_{1-c}Ge_c$ nanowires (reverse heat flux), from $c = 0$ at $z = 0$ to $c = 1$ al $z = L$ in order to explore the consequences of several physical factors on the value of the rectification coefficient $R[c(z), T_H, T_C]$ going beyond the simplified situations analyzed in Refs. [4,20]. In fact, we explore the influence on R of the constitutive equation (1) for the thermal conductivity, of the spatial composition profile $c(z)$, of the value of the direct heat flux q_d, and of the length of the system L. To obtain the rectification coefficient, we must calculate the temperature profiles in the direct situation (heat flux from Ge to Si or, equivalently, heat flux in Si_cGe_{1-c}) and in the reverse situation (heat flux from Si to Ge or, equivalently, heat flux in $Si_{1-c}Ge_c$), by:

(1) applying T_H (hottest T) and a given q_d on the Ge side, and obtaining the corresponding lowest temperature T_C at the Si side (direct situation);
(2) applying T_H on the Si side and trying for different values of q_r until finding the value q_r for which the temperature at the Ge side is the lowest temperature T_C previously obtained for q_d (reverse situation).

The temperature profiles are obtained in steady state, under the hypothesis of validity of the Fourier law

$$q = -\lambda(T, c)\frac{dT}{dz}, \tag{5}$$

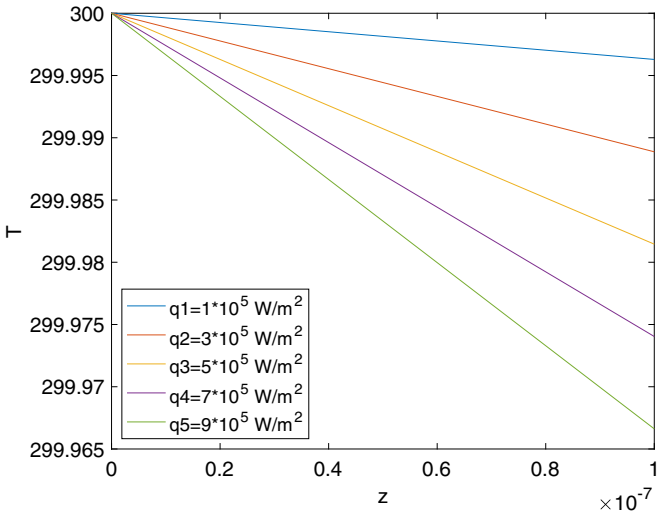

(a) From Ge to Si (direct flux)

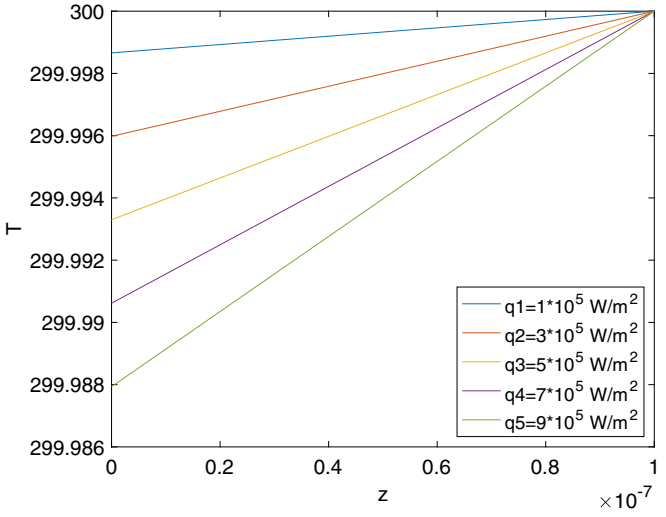

(b) From Si to Ge (reverse flux)

Fig. 2. Temperature profile for a linear composition profile $c(z) = z/L$, from $c = 0$ to $c = 1$, for q from 1×10^5 Wm^{-2} to 9×10^5 Wm^{-2} (as indicated in the figure) and L = 100 nm.

with a superimposed heat flux q_d, which will be constant along the one-dimensional system in steady state, because of the condition $\nabla \cdot \mathbf{q} = 0$. In this situation, we obtain the temperature profile by solving the differential equation

$$\frac{dT}{dz} = -\frac{q}{\lambda(T(z), c(z))}, \tag{6}$$

with $\lambda(T(z), c(z))$ given by Eq. (1) and with given composition profile $c(z)$.

In the direct situation Si_cGe_{1-c}, we have considered that Ge ($c = 0$) is at the hot side ($z = 0$) (at 300 K) and Si ($c = 1$) is at the cold side ($z = L$). In the reverse situation $Si_{1-c}Ge_c$, instead, we have considered that Si ($c = 0$) is at the hot side ($z = 0$) and Ge ($c = 1$) is at the cold side ($z = L$). Indeed, we have assumed that the hot side is always at the left ($z = 0$), and that in the direct case pure Ge is at $z = 0$, while in the reverse case pure Si is at $z = 0$. In Fig. 2 we plot the temperature profiles corresponding to different values of the heat flux, for heat going from Ge to Si (direct case) Fig. 2(a), or from Si to Ge (reverse case) Fig. 2(b), always with $T = 300$ K

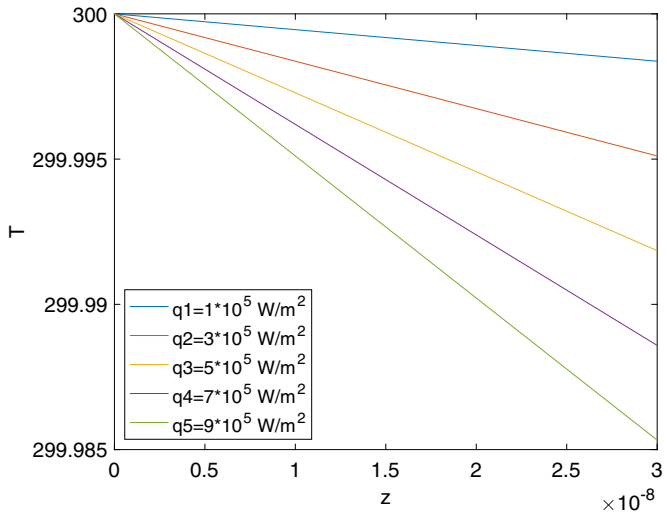

(a) From Ge to Si (direct flux)

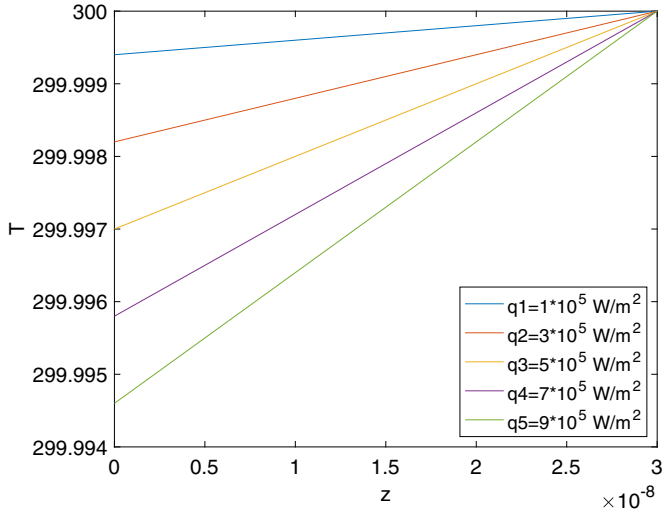

(b) From Si to Ge (reverse flux)

Fig. 3. Temperature profile for a linear composition profile $c(z) = z/L$, from $c = 0$ to $c = 1$, for q from 1×10^5 Wm^{-2} to 9×10^5 Wm^{-2} (as indicated in the figure) and L = 30 nm.

at the hottest side (left side, $z = 0$) and for a linear composition profile, namely $c(z) = z/L$, with $z \in [0, L]$, and L = 100 nm. On the right-hand side of the figures are shown the values of T_C corresponding to different values of the direct heat flux. In Fig. 3 we plot the temperature profiles corresponding to different values of the heat flux, for heat going from Ge to Si (direct case) Fig. 3(a), or from Si to Ge (reverse case) Fig. 3(b), always with $T = 300$ K at the hottest side (left side, $z = 0$) and for a linear composition profile, namely $c(z) = z/L$, with $z \in [0, L]$, and L = 30 nm. Nonlinear composition profiles, namely $c(z) = (z/L)^2$, $c(z) = (z/L)^3$, could also be considered by using the same method as above. In future works, we intend to analyze and compare these cases with the linear composition profile.

3.2. Rectification coefficient

Once the temperature profiles have been obtained, the rectification coefficient can be calculated by the mathematical procedure illustrated by the items 1) and 2) above. In Tables 10 and 11,

Table 10
Rectification coefficient for linear composition profiles, $c(z) = z/L$, for different values of the direct heat flux from 1×10^5 Wm^{-2} to 9×10^5 Wm^{-2}. The T_H and T_C highest and lowest boundary temperatures are also indicated and L = 100 nm.

q_d	R	T_H	T_C
1×10^5	2.77/1 = 2.7700	300	299.9963
3×10^5	8.30/3 = 2.7667	300	299.9889
5×10^5	13.8/5 = 2.7600	300	299.9815
7×10^5	19.365/7 = 2.7664	300	299.9740
9×10^5	24.9/9 = 2.7667	300	299.9666

Table 11
Rectification coefficient for linear composition profiles, $c(z) = z/L$, for different values of the direct heat flux from 1×10^5 Wm^{-2} to 9×10^5 Wm^{-2}. The T_H and T_C highest and lowest boundary temperatures are also indicated and L = 30 nm.

q_d	R	T_H	T_C
1×10^5	2.718/1 = 2.7180	300	299.9984
3×10^5	8.15/3 = 2.7167	300	299.9951
5×10^5	13.6/5 = 2.7200	300	299.9918
7×10^5	19/7 = 2.7143	300	299.9886
9×10^5	24.46/9 = 2.7178	300	299.9853

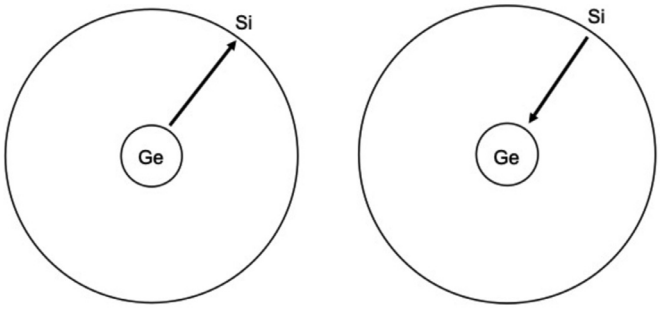

(a)From Ge to Si (b)From Si to Ge

Fig. 4. Direct and reverse heat flow for Ge inside and Si outside.

we show the corresponding values of the rectification coefficient for linear composition profile $c = z/L$, for different values of the direct heat flux from 1×10^5 Wm^{-2} to 9×10^5Wm^{-2}, both for L = 100 nm and L = 30 nm. It can be seen that R is almost independent of the intensity of the direct heat flux, and is a little bit higher for L = 100 nm. However, we observe that R is very high, and this result confirms the good performance of graded materials as thermal rectifiers.

4. Rectification in cylindrical nanodevices

4.1. Fourier law in cylindrical coordinates

In this section we consider a cylindrical system with axial symmetry, undergoing radial heat flow along the direction r, and $r \in [r_{int}, r_{ext}]$ with r_{int} and r_{ext} being the internal and external radii. We combine such a geometry with graded Si_cGe_{1-c} composition, where c depends linearly on r, namely $c(r) = \dfrac{r - r_{\text{int}}}{r_{\text{ext}} - r_{\text{int}}}$. We will consider the direct and reverse heat flow in the following situations:

- Ge inside Si outside (Fig. 4);
- Si inside Ge outside (Fig. 5).

We will denote as direct heat flux q_d the outward one, and as reverse heat flux q_r the inward one. In these situations the differ-

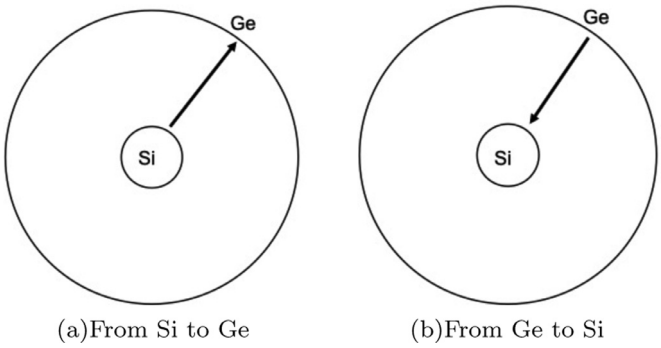

Fig. 5. Direct and reverse heat flow for Si inside and Ge outside.

Table 12
Rectification coefficient for linear profile $c(r) = \frac{r - r_{int}}{r_{ext} - r_{int}}$, for different values of the direct heat flux in the range of $10^9 Wm^{-2}$, for $r_{int} = 50$ nm and $r_{ext} = 150$ nm.

Γ	R	T_H	T_C
2×10^2	$2.82272/2 = 1.4114$	300	250.5158
4×10^2	$5.642145/4 = 1.4105$	300	201.3330
6×10^2	$8.460195/6 = 1.4100$	300	152.3789
8×10^2	$11.278775/8 = 1.4098$	300	103.5833

ence in the value of the internal and external radii acts as a further inhomogeneity of geometrical kind, which may enhance or reduce the effects of the material inhomogeneity in the concentration. Indeed, in the heat flow along a nanowire, the two situations described above (Ge inside, Ge outside) would be equivalent, since they would correspond to having pure Ge on the left hand side or on the right hand side of the nanowire, and it would be inconsequential for the value of the rectification. In the axial case, instead, they become physically differentiated, because of the geometry (the area corresponding to Ge in the cases Ge inside and Ge outside is no longer the same one).

In this geometry, the Fourier law takes the form

$$q = \frac{\Gamma}{r} = -\lambda(T(r), c(r))\frac{dT}{dr}, \tag{7}$$

where Γ is a constant (proportional to the total heat per unit time supplied to the system per unit length of the cylinder). The form of q in (7) follows by the equation $\nabla \cdot \mathbf{q} = 0$ (steady state condition) which, in polar coordinates and in the presence of radial symmetry, leads to $q(r) \sim 1/r$. Thus, the temperature profile will be found by solving the differential equation

$$\frac{dT}{dr} = -\frac{\Gamma}{\lambda(T(r), c(r))r}. \tag{8}$$

We take Γ of order of magnitude 10^2 Wm^{-1}, in order to have a heat flux of order of magnitude 10^9 Wm^{-2} for $r \in [100\,nm, 150\,nm]$, and a heat flux of order of magnitude 10^{10} Wm^{-2} for $r \in [10\,nm, 40\,nm]$.

4.2. Rectification coefficient in cylindrical geometry

In Table 12, we give the values of the rectification coefficient for $c(r) = \frac{r - r_{int}}{r_{ext} - r_{int}}$, with $r_{int} = 50$ nm and $r_{ext} = 150$ nm (from Ge to Si direct case, from Si to Ge reverse case).

In Table 13, we give the values of the rectification coefficient for $c(r) = \frac{r - r_{int}}{r_{ext} - r_{int}}$, with $r_{int} = 50$ nm and $r_{ext} = 150$ nm (from Si to Ge direct case, from Ge to Si reverse case).

Table 13
Rectification coefficient for linear profile $c(r) = \frac{r - r_{int}}{r_{ext} - r_{int}}$, for different values of the direct heat flux in the range of $10^9 Wm^{-2}$, for $r_{int} = 50$ nm and $r_{ext} = 150$ nm.

Γ	R	T_H	T_C
2×10^2	$3.8011/2 = 1.9005$	300	288.6905
4×10^2	$7.60195/4 = 1.9005$	300	277.3863
6×10^2	$11.4029/6 = 1.9005$	300	266.0857
8×10^2	$15.2043/8 = 1.9005$	300	254.7868

Table 14
Rectification coefficient for linear profile $c(r) = \frac{r - r_{int}}{r_{ext} - r_{int}}$, for different values of the direct heat flux in the range of $10^{10} Wm^{-2}$, for $r_{int} = 10$ nm and $r_{ext} = 40$ nm.

Γ	R	T_H	T_C
2×10^2	$2.77405/2 = 1.3870$	300	263.0657
4×10^2	$5.536585/4 = 1.3841$	300	226.7908
6×10^2	$8.28525/6 = 1.3809$	300	191.2387
8×10^2	$11.01813/8 = 1.3773$	300	156.4585

Table 15
Rectification coefficient for linear profile $c(r) = \frac{r - r_{int}}{r_{ext} - r_{int}}$, for different values of the direct heat flux in the range of $10^{10} Wm^{-2}$, for $r_{int} = 10$ nm and $r_{ext} = 40$ nm.

Γ	R	T_H	T_C
2×10^2	$3.46703/2 = 1.7335$	300	290.5539
4×10^2	$6.93557/4 = 1.7339$	300	281.0937
6×10^2	$10.40599/6 = 1.7343$	300	271.6178
8×10^2	$13.87859/8 = 1.7348$	300	262.1244

In Table 14, we give the values of the rectification coefficient for $c(r) = \frac{r - r_{int}}{r_{ext} - r_{int}}$, with $r_{int} = 10$ nm and $r_{ext} = 40$ nm (from Ge to Si direct case, from Si to Ge reverse case).

In Table 15, we give the values of the rectification coefficient for $c(r) = \frac{r - r_{int}}{r_{ext} - r_{int}}$, with $r_{int} = 10$ nm and $r_{ext} = 40$ nm, (from Si to Ge direct case, from Ge to Si reverse case).

Although smaller with respect to that of the linear case, the rectification coefficient corresponding to the cylindrical case is also very high and independent of the intensity of the applied heat flux. Moreover, also in this case, it seems to increase with the length of the system.

5. Concluding remarks

In the present paper the analysis developed in Ref. [5] has been applied by using a different constitutive equation for the thermal conductivity, i.e., Eq. (1), which has been obtained by determining a mathematical fit of the experimental results [21]. It is seen that the value of R in the full range $0 \le c \le 1$ is higher than 2.7 (Tables 10 and 11), thus indicating a meaningful rectification, both for nanowires of length L = 100 nm, and of length L = 30 nm. For cylindrical systems with transversal section of radius $r_{int} = 50$ nm and $r_{ext} = 150$ nm, we got $R \simeq 1.41$ if we have the direct case from Ge to Si and the reverse case from Si to Ge, and $R \simeq 1.90$ if we have the direct case from Si to Ge, and the reverse case from Ge to Si (Tables 12 and 13). For cylindrical systems with transversal section of radius $r_{int} = 10$ nm and $r_{ext} = 40$ nm, we got $R \simeq 1.38$ if we have the direct case from Ge to Si and the reverse case from Si to Ge, and $R \simeq 1.73$ if we have the direct case from Si to Ge and the reverse case from Ge to Si (Tables 14 and 15). The results above

denote a meaningful improvement of the rectification coefficient, both for linear and cylindrical systems, with respect to the results obtained in [5]. In future researches we plan to analyze the same problem for the bulk, namely, for L in the interval [1 mm, 4 mm]. Indeed, for such a length the function in Eq. (1) does not seems to fit the experimental data with the same precision of nanometric scale and some improvement seems to be necessary. We also plan to explore composition spatial distribution non linear in the position (namely $c(z) = (z/\mathrm{L})^a$), with a an exponent and composition ranges from $c = 0$ to 0.1, and $c = 0.9$ to 1. Finally, we remark that the results above have been obtained under the hypothesis of validity of the classical Fourier's law. However, one can find in literature several theories of heat conduction beyond the Fourier's law [22–25]. For instance, in Extended Irreversible Thermodynamics [24,26,27], the heat flux is no longer assigned by a constitutive equation but is determined by a suitable balance law [24,26–29]. Thus, it would be interesting to explore, for different geometries, the influence on R of the additional term $\ell^2\nabla^2\mathbf{q}$ with ℓ as the mean free path of phonons in the expression of the heat flux. Moreover, for materials of the type considered here, it is interesting to investigate how ℓ changes with c, and determine a suitable law of dependence on c.

Declaration of Competing Interests

The authors declare that they have no known competing financial interests or personal relationships that could have appeared to influence the work reported in this paper.

Acknowledgements

I. C. acknowledges the financial support from Italian Gruppo Nazionale per la Fisica Matematica (GNFM-INδAM). V. A. C. acknowledges the financial support from the Italian Gruppo Nazionale per la Fisica Matematica (GNFM-INδAM), and from the University of Basilicata under grants RIL 2013 and RIL 2015. D. J. acknowldges the financial support of Ministerio de Economía y Competitividad of the Spanish Government under grant RTI 2018-097876-B-C22 and of the Direcció General de Recerca of the Generalitat de Catalunya under grant 20175GR-1018.

References

[1] H. Sadat, V.L. Dez, On the thermal rectification factor in steady heat conduction, Mech. Res. Commun. 76 (2016) 48–50.
[2] Y. Gelbstein, Z. Dashevsky, M. Dariel, High performance n-type PbTe-based materials for thermoelectric applications, Physica B 363 (2005) 196–205.
[3] Y. Gelbstein, Z. Dashevsky, M.P. Dariel, Powder metallurgical processing of functionally graded p-$Pb_{1x}Sn_x$Te materials for thermoelectric applications, Physica B 391 (2007) 256–265.
[4] D. Jou, I. Carlomagno, V.A. Cimmelli, A thermodynamic model for heat transport and thermal wave propagation in graded systems, Physica E 73 (2015) 242–249.
[5] I. Carlomagno, V. Cimmelli, D. Jou, Heat flux rectification in graded Si_cGe_{1-c}: longitudinal and radial heat flows, Physica E 90 (2017) 149–157.
[6] A.O. Olatunji-Ojo, S.K.S. Boetcherb, T.R. Cundaria, Thermal conduction analysis of layered functionally graded materials, Comput. Mater. Sci. 54 (2012) 329–335.
[7] N. Li, J. Ren, L. Wang, G. Zhang, P. Hänggi, B. Li, Colloquium: Phononics: Manipulating heat flow with electronic analogs and beyond, Rev. Mod. Phys. 84 (2012) 1045–1066.
[8] M. Maldovan, Sound and heat revolutions in phononics, Nature 503 (2013) 209–217.
[9] S.R. Sklan, Splash, pop, sizzle: Information processing with phononic computing, AIP Adv. 5 (2015) 053302.
[10] L. Wang, B. Li, Phononics gets hot, Physics World 21 (2008) 27–29.
[11] D. Sawaki, W. Kobayashi, Y. Moritomo, I. Terasaki, Thermal rectification in bulk materials with asymmetric shape, Appl. Phys. Lett. 98 (2011) 081915.
[12] N. Yang, G. Zhang, B. Li, Carbon nanocone: A promising thermal rectifier, Appl. Phys. Lett. 93 (2008) 243111.
[13] M. Criado-Sancho, L.F.D. Castillo, J. Casas-Vázquez, D. Jou, Theoretical analysis of termal rectification in a bulk Si/nanoporous Si device, Phys. Lett. A 376 (2012) 1641.
[14] M. Criado-Sancho, F.X. Alvarez, D. Jou, Thermal rectification in inhomogeneous nanoporous Si devices, J. Appl. Phys. 114 (2013) 053512.
[15] E. González-Noya, D. Srivastava, M. Menon, Heat-pulse rectification in carbon nanotube Y junctions, Phys. Rev. B 79 (2009) 115432.
[16] C. Glassbrenner, G. Slack, Thermal conductivity of silicon and germanium from 3° K to the melting point, Phys. Rev. 134 (1964) 1058–1069.
[17] M. Steele, F. Rosi, Thermal conductivity and thermoelectric power of germanium-silicon alloys, J. Appl. Phys. 29 (1958) 1517–1520.
[18] B. Abeles, D. Beers, G. Cody, J. Dismukes, Thermal conductivity of Ge-Si alloys at high temperatures, Phys. Rev. 125 (1962) 44–46.
[19] B. Abeles, Lattice thermal conductivity of disordered semiconductor alloys at high temperatures, Phys. Rev. 131 (1963) 1906–1911.
[20] I. Carlomagno, V.A. Cimmelli, D. Jou, Computational analysis of heat rectification in composition-graded systems: From macro-to-nanoscale, Physica B 481 (2016) 244–251.
[21] P. Rogolino, V.A. Cimmelli, Fitting thermal conductivity and optimizing thermoelectric efficiency of functionally graded Si_cGe_{1-c} nanowires, Math. Comput. Simulation (2019), doi:10.1016/j.matcom.2019.09.020. Article in press
[22] V.A. Cimmelli, Different thermodynamic theories and different heat conduction laws, J. Non-Equilib. Thermodyn. 34 (2009) 299–333.
[23] G. Lebon, Heat conduction at micro and nanoscales: A review through the prism of Extended Irreversible Thermodynamics, J. Non-Equilib. Thermodyn. 39 (2014) 35–59.
[24] V.A. Cimmelli, D. Jou, T. Ruggeri, P. Ván, Entropy principle and recent results in non-equilibrium theories, Entropy 16 (2014) 1756–1807.
[25] S. Both, B. Czél, T. Fülöp, G. Gróf, A. Gyenis, R. Kovács, P. Ván, J. Verhás, Deviation from the Fourier law in room-temperature heat pulse experiments, J. Non-Equilib. Thermodyn. 41 (2016) 41–48.
[26] D. Jou, J. Casas-Vázquez, G. Lebon, Extended irreversible thermodynamics, Berlin, Springer, 2010. (Fourth edition)
[27] G. Lebon, D. Jou, J. Casas-Vázquez, Understanding non-equilibrium thermodynamics, Berlin, Springer, 2008.
[28] P. Jordan, W. Dai, R.E. Mickens, A note on the delayed heat equation: Instability with respect to initial data, Mech Res. Commun. 35 (2008) 414–420.
[29] R. Quintanilla, P.M. Jordan, A note on the two temperature theory with dual-phase–lag delay: Some exact solutions, Mech. Res. Commun. 36 (2009) 796–803.